

# Encounters with Vortices in a Turbine Nozzle Passage

J. P. Gostelow<sup>1,2</sup>, A. Mahallati<sup>1</sup>, W. E. Carscallen<sup>1</sup>, A. Rona<sup>2</sup>

<sup>1</sup> Institute for Aerospace Research,  
 National Research Council of Canada, Ottawa, K1A 0R6, Canada

<sup>2</sup> University of Leicester, Leicester, LE1 7RH, UK

Corresponding author: Professor J.P. Gostelow, GTL, IAR, M-10, National Research Council, Ottawa, K1A 0R6, Canada. Phone: +1 (613) 990 1133. Fax: +1 (613) 952 7677. Email: Paul.Gostelow@nrc.ca

## ABSTRACT

Experiments were conducted on the flow through a transonic turbine cascade. A wide range of vortices was encountered including horseshoe vortices, secondary flows, shock-induced passage vortices and streamwise vortices on the suction surface. In the separation region on the suction surface, a large roll-up of passage vorticity occurred. The blunt leading edge gave rise to strong horseshoe vortices and secondary flows. The suction surface had a strong convex curvature over the forward portion and was quite flat further downstream. Surface flow visualization was performed and this convex surface displayed coherent streamwise vorticity. At subsonic speeds strong von Kármán vortex shedding resulted in a substantial base pressure deficit. For these conditions time-resolved measurements were made of Eckert-Weise energy separation in the blade wake. At transonic speeds, exotic shedding modes were observed. These phenomena all occurred in experiments on the flow around one particular turbine nozzle vane in a linear cascade.

## NOMENCLATURE

$C_p$	Static pressure coefficient
$D$	Diameter of cylinder
$M_e$	Exit isentropic Mach number
$P$	Pressure
$PR$	Pressure ratio
$Re$	Reynolds number
$Tu$	Free-stream turbulence level, %
$t$	Time
$y$	Normal direction
$\lambda$	Spanwise wavelength

## Subscripts

$b$	Base value
$s$	Static condition
$0$	Stagnation condition

## INTRODUCTION

Leonardo da Vinci (1506-1510) was a notable early observer of vortices produced by a solid object placed in a stream of flow (Fig. 1). When the object has thickness and produces a flow turning of 70° or more, the generation of strong vorticity is to be expected and the subject turbine nozzle blading is no exception. The different vortical phenomena arising in the flow passage are described in this paper. The variety of the vortical forms and occurrences is surprising.

The encounters with vortices involve the flows outlined in the paper, starting at the leading edge. These are horseshoe vortices, secondary flows, passage vortices and, on the suction surface, streamwise vortices. At the trailing edge, vortex shedding, energy separation, base pressures, and exotic shedding modes are observed. This is all in experiments on the flow around one particular turbine nozzle vane in a linear cascade. This diversity of vortex phenomena illustrates the challenge of describing the fundamental internal aerodynamics of turbomachinery blading. Greater physical understanding is required of these phenomena, including vortex structures on surfaces, vortex shedding, the base region, the vortex wake and its interaction with the shock waves.

Surface flow visualization was performed on the suction surface of the turbine blade at subsonic and transonic speeds. This was effective in providing a time-average mapping of streamwise vortical structures within the blade passage. Under the influence of the strong favorable pressure gradients on the suction surface, the vortices were remarkably persistent, lasting to the trailing edge.



Fig. 1 Observations of vortices by Leonardo da Vinci.

Previous investigators have observed streamwise vortices and “streaky structures” on flat plates and on the suction surface of compressor blades. Turbine blade designers are quite familiar with the phenomenon of Görtler vorticity; this is commonly thought to occur predominantly on the concave pressure surfaces of turbine blades. An organized streamwise vortex system tends to increase heat transfer to the blade surface and also makes the flow and heat transfer difficult to predict. Designers generally assume that streamwise vorticity of this kind is confined to the concave pressure surfaces. Examples will be given which should result in a questioning of the assumption that organized streamwise vorticity is confined to the pressure surface of a turbine blade.

Although it appears to be unusual, this behavior had been predicted and observed previously with attendant theories for wavelength. For a predominantly convex surface, the behavior is consistent with the later predictions of Görtler (1955), who postulated instability on a convex surface from the concave streamlines ahead of the leading edge stagnation region. Measurements of spanwise wavelength of the periodic array of vortices are found to be compatible with the subsequent predictions of Kestin and Wood (1970).

In the mid nineteen-seventies a National Research Council / Pratt and Whitney, Canada collaborative program was established to produce a gas generator with a turbine stage of aggressive design. The turbine was highly loaded, giving a low wheel speed. This was supported by a Highly Loaded Turbine Test Facility that was of three times PT6 engine size and matched the engine Mach and Reynolds numbers. The turbine nozzle had a thick trailing edge to allow for cooling passages (Williamson and Moustapha, 1986).

The stage employed a high turning transonic nozzle and was tested over a range of exit Mach numbers between 0.67 and 1.2. During testing, this turbine stage gave some inexplicable results that showed a redistribution of the downstream total temperature field. In this ostensibly adiabatic arrangement, the central regions of the vane wakes exhibited a significant decrease in total temperature and their edges showed an unexpected increase.

To resolve these anomalous results and obtain detailed information over the Mach number range, the midspan section of the nozzle was tested in a large scale, low aspect ratio, transonic planar cascade (Carscallen and Oosthuizen, 1988). Some details of the blading are given in Fig. 2. At high subsonic speeds, acoustically-coupled vortex shedding created energy redistribution in the wake. This was measured using wide bandwidth temperature probes. In the first time-resolved measurements of wake temperature redistribution, by Carscallen et al. (1999), the vortex shedding was shown to give rise to an effect first noted by Eckert and Weise (1943). This had led to problems in the development of an advanced turbine stage.

- 6 Airfoils (5 passages)
- Mid-span of a HPT vane
- 4.3 times engine size
- Correct engine  $Re$  of  $2.13 \times 10^5$
- Correct engine  $M_e$  of 1.16 at a  $PR$  of 2.3
- Stagger angle  $64^\circ$
- Solidity 1.19

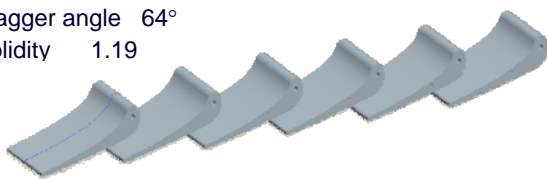


Fig. 2 Some features of the blading.

Base pressures are also associated with vortex shedding and result in increased drag for bluff bodies and turbine blades. Time-resolved pressure distributions gave information on fluctuations and corresponding base drag coefficients.

The most common shedding mode is not the only mode. Not all vortex shedding takes the form of the classical vortex street described by von Kármán; a wide range of ‘exotic’ modes also exists. The discovery of these anomalous patterns behind transonic turbine blades was first reported to ISROMAC-5 by Carscallen and Gostelow (1994) and resulted in an investigation into when they might occur. Two other applications were found in the vortex-induced vibration of bluff bodies and research on oscillating airfoils. Findings from the vortex-induced vibration work of Williamson and Roshko (1988) have clarified the shedding modes.

## PASSAGE VORTICES

The inlet wall boundary layer occupies 10% of the span and the leading edge was thick and blunt, giving rise to strong horseshoe vortices and secondary flows. The secondary flow creates a large displacement which affects the streamlines well outside the secondary flow zones. When applied to the flow in a cascade the term ‘secondary flow’ is restricted to the differential deflection imparted by the cascade, to a sheared free stream. In this case, the principal source of shear at inlet is the wall boundary layer.

At the mid-span, the surface streamlines are all parallel and the flow appears to be two-dimensional. At Mach 1.16 the shock impingement and separation region is associated with a strong vortex roll-up where the shock impingement meets the side-wall boundary layer. This is associated with the passage vortex.

Two other vortex types should be mentioned. These are the relatively small contra-rotating corner vortex and the rather larger wall vortex that is induced by the passage vortex.

The small ‘corner vortex’ is present beneath the larger multi-vortex structure. It has an induced sense of rotation contrary to that of the main passage vortex. This vortex resides in the corners between the endwalls and the pressure and suction surfaces.

A rather larger contra-rotating vortex, adjacent to the end wall, is induced by the impingement of the main passage vortex on the suction surface of the blade. This ‘wall vortex’ tends to scrub the endwall in the downstream mid-passage region. It moves away from the suction surface toward the mid-passage region between the suction and pressure surfaces.

## Horseshoe Vortices

Surface flow visualization was applied, with the aim of establishing the strength of the leading edge horseshoe vortex.

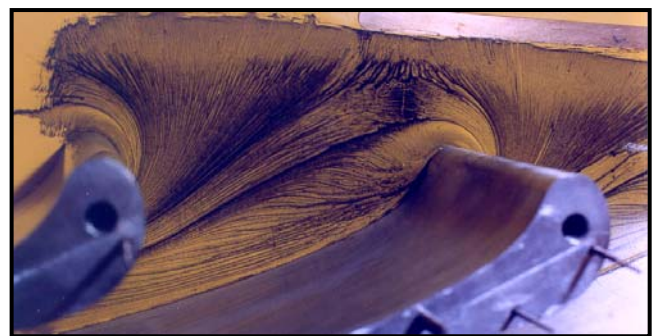


Fig. 3 End-wall visualization of horseshoe vortex.

This demonstrated that on the end walls the influence of the horseshoe vortex was very strong, as shown in Fig. 3. The principal horseshoe vortex around the leading edge had both pressure surface and suction surface components. The pressure surface leg was swept over toward the suction surface, eventually to become the main passage vortex. The static pressure gradient acting on this vortex leg is the same at the end wall as that in the free stream but the velocity is lower in the end wall region. The radius of curvature of the streamlines in the sidewall region must also be lower to preserve radial equilibrium. The path the vortex takes in the end wall region therefore has high curvature and this accounts for its rapid movement across the passage.

### Passage Vortices

A qualitative measure of vortex structure, on a time averaged basis, was obtained using surface oil-flow visualization (Gostelow et al., 2009). The blade was covered with a sheet of self-adhesive white vinyl. A mixture of artist grade linseed oil and powdered lampblack shaded pigment was applied in a very thin and uniform layer over the suction surface. After letting the tunnel run for about five minutes, the blade was removed and photographed.

Inside the primary passage vortex the mean pressure fluctuations and resolved kinetic energy levels are large. The maximum shear levels are observed beneath the main passage vortex and close to the small corner vortices. The visualization of the suction surface flow at  $M_e = 1.16$  is shown in Fig. 4. The large numbers on the scale represent percentage axial chord and the small numbers mark static tap locations. The shock impingement and separation region is around the 70% axial chord location.

There was a strong vortex roll-up where the impinging shock met the side-wall boundary layer. The sense of rotation and the direction of the back flow into the separated region following the shock can be deduced. Rotation was counter-clockwise on the left hand side and clockwise on the right hand side of the vane.

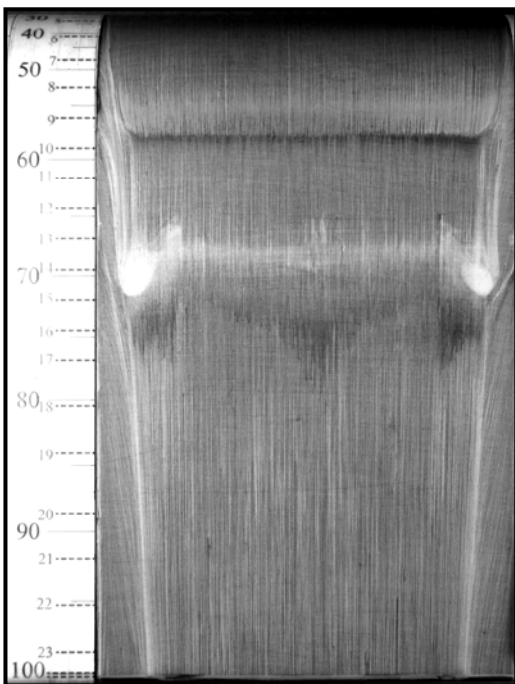


Fig. 4 Visualization of suction surface at  $M_e = 1.16$ .

A close-up view of the vortex formed in the vicinity of the impinging shock, and of the resulting separation region, is given in Fig. 5. The sense of rotation, and of the resulting back flow into the separated region following the shock, are shown clearly. Fine scale streamwise vortices also show up in Fig. 5. For a predominantly convex surface this behavior was unexpected. At the leading edge the suction surface is virtually circular; subsequently, much of the suction surface retains a strong convex curvature over the forward portion and is quite flat further downstream. Surface flow visualization was performed at subsonic and transonic speeds and the surface displayed coherent streamwise vorticity covering the entire surface to the trailing edge.

### Streamwise Vortices

Surface flow visualization was performed at subsonic and transonic speeds and the suction surface displayed coherent streamwise vorticity extending to the trailing edge. A close-up view of the visualization from a discharge Mach number of 1.16 is given in Fig. 6. A region between about 80% and 95% axial chord is presented. Fine scale streamwise vortices show up clearly in the figure. For a predominantly convex surface this behavior is unexpected but is in agreement with the later predictions of Görtler (1955), who postulated instability on a convex surface from the concave streamlines ahead of the leading edge stagnation region.

The measurements of the spanwise wavelength of the array of vortices may be compared with the predictions of Kestin and Wood (1970). They predicted a theoretical value of spanwise wavelength between pairs,  $\lambda$ , for a cylinder of diameter,  $D$ , given by:

$$\lambda = 1.79\pi D Re^{-0.5}. \quad (1)$$

It is difficult to locate this case on the Kestin and Wood graph as Eq. (1) represents flow past a circular cylinder. The leading edge of the turbine blade is relatively blunt but nevertheless has a high surface curvature which decreases rapidly to near zero further back.

The rapid changes in curvature of the convex surface raise the question of what effective diameter should be applied if comparing with the Kestin and Wood model. According to the Kestin and Wood theory, the measured wavelength, of 0.55 mm, is compatible with the curvature of the suction surface at approximately the 10%

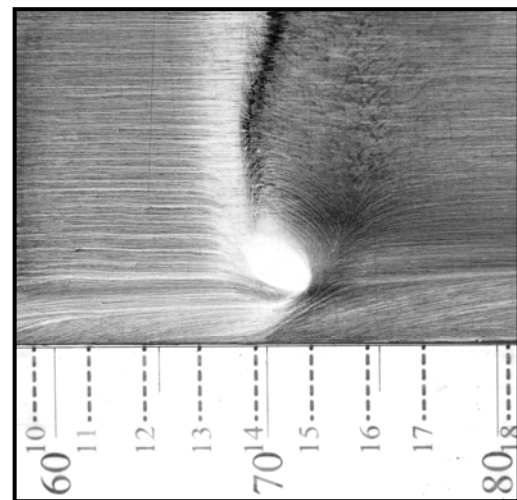
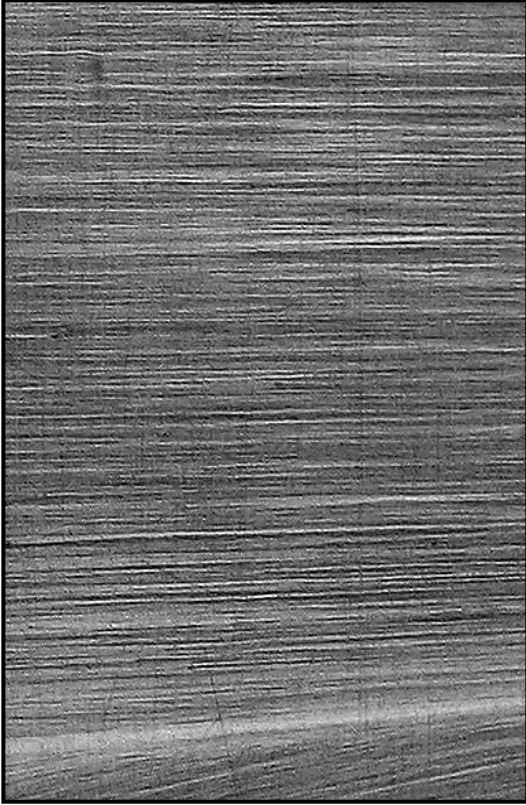


Fig. 5 Enlarged view of the vortex on the suction surface.





**Fig. 6 Close-up visualization of streamwise vortices.**

true chord location (Fig. 7). Because the geometry is quite different from that of a circular cylinder, only qualitative agreement with the predictions can be expected and that is what was achieved. However, surface flow visualization photographs have been analyzed from the work of a number of published experiments. When examined in the same way as the results of Fig. 6, two results from compressor blading (Schulz and Gallus, 1988, and Weber et al., 2002) and two from turbine blading (Benner et al., 1997, and Hodson and Dominy, 1987) are available and also give reasonable agreement with the theory and experiments of Kestin and Wood (Fig. 7). The free-stream turbulence levels for the above cases were all in the range  $0.2\% \leq Tu \leq 1.2\%$ .

For the subject blading, the acceleration through the passage is strong. The mass averaged inlet Mach number at the design condition is 0.118 whilst the discharge Mach number is 1.16, giving an order of magnitude difference. It is the flow in the vicinity of the leading edge that determines the susceptibility of the flow to organized streamwise vorticity and, at a local Mach number of 0.118, the flow dynamics should not be very different from previous observations that were undertaken in low speed flows.

In assessing the results, it should be borne in mind that the Mach number regime and model geometry differ from others considered in the published literature. The blades have a very blunt leading edge and are therefore likely candidates to experience flow instability upstream of the stagnation point and the consequent streamwise vorticity. One outcome of these investigations is to establish that organized streamwise vorticity may occur more frequently on convex surfaces, such as turbine blade suction surfaces, than was previously appreciated. Investigations

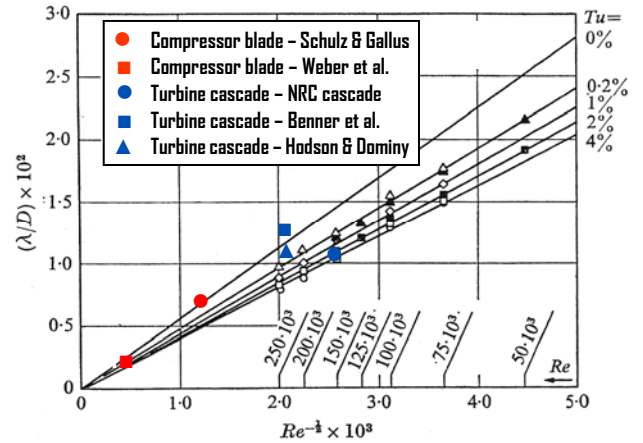


**Fig. 7 Measurements of wavelength and comparison with Kestin and Wood predictions.**

and predictions of flow behavior should be extended to encompass this possibility. If this behavior is at all common, it could have interesting implications for turbine aerodynamic and blade cooling design.

## SHED VORTICES

Turbomachinery blades with thick trailing edges, such as those investigated by Carscallen et al. (1996), are associated with a high loss penalty. This loss penalty is greater than would be expected from a simple backwards-facing step and remained unexplained until high speed Schlieren photography was applied to cascades (Lawaczeck and Heinemann, 1976).

Vortex shedding is present in the wakes of blades with thick trailing edges (Fig. 8) and the unexplained losses are clearly associated with the shedding process. Among other problems, this drastically increases the base drag at subsonic speeds. In addition to the loss penalty, vortex shedding may cause adverse effects including high frequency sound propagation, vibration effects, locally high heat transfer to or from the blade surface and energy separation into hot and cold regions. The vortex street, often with closely coupled oscillating shock waves, jeopardizes RANS flow field computations.

Nevertheless with modern CFD approaches these difficulties can be overcome. An instantaneous view from an unsteady RANS calculation for the cascade investigated is given in Fig. 9. The interactions between shed vortices and oscillating shock waves are quite complex but have been handled well by the code.

Experimental results for the blade Mach number distribution and computational predictions are given, with the blade layout, in Fig. 10. The agreement between computation and experiment is seen to be reasonable.

## Base Pressures

Another detrimental flow phenomenon affected by vortex shedding in turbomachinery is base pressure. It has long been realized that turbomachinery blades with thick trailing edges have an area of reduced static pressure around the trailing edge that creates a considerable increase in base drag at subsonic speeds and reduces the stage efficiency. Cicatelli and Sieverding (1996)

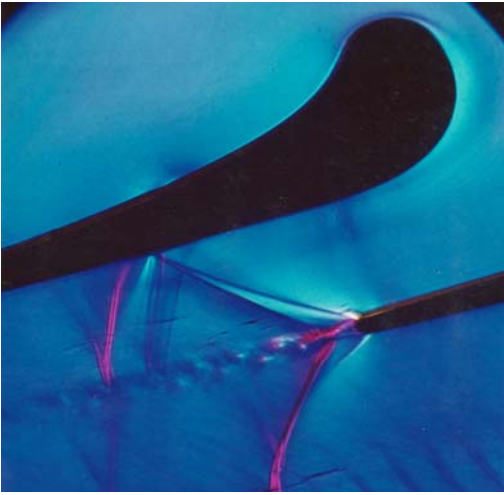


**Fig. 8 Schlieren view of vortex shedding at  $M_e = 1.16$ .**

conducted an investigation into the effect of vortex shedding on the base region flow. They found that the pressure in this region fluctuated by as much as 8% of the downstream dynamic head near separation, and by 4.8% in the base region.

It is clear that the instantaneous base pressure could be significantly different from the time-averaged value. Computations for blading designed using steady state methods will be erroneous for much of the vortex shedding cycle.

At subsonic speeds strong suction at the trailing edge is an essential facet of the vortex shedding process that results in increased drag for bluff bodies and turbine blades. The pressure distribution around a cylinder depends strongly on Mach number. Time-resolved pressure distributions give information on fluctuations and corresponding drag coefficients. Base pressures were measured at the extreme trailing edge of the blades.

The values obtained are plotted in Fig. 11 and the base pressure deficit is seen to reach a maximum at a discharge Mach number of 0.9. The results are supplemented by earlier results obtained by Carscallen et al. (1996). The results exhibit scatter due to unsteadiness but are basically quite similar.

Base pressure is an important contributor to the turbine stage total loss. Work by Denton (1993) and by Mee et al. (1992) showed the base pressure contributing a significant proportion of the total loss at high speeds. Carscallen et al. (1996) found that the lowest base pressure was accompanied by the strongest vortex shedding.

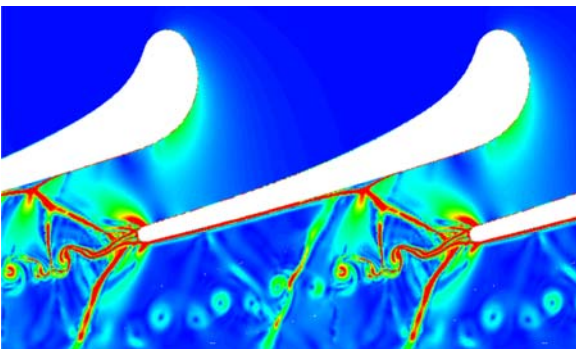


**Fig. 9 Instantaneous CFD view of vortex shedding/ shock wave interaction at  $M_e = 1.16$ .**

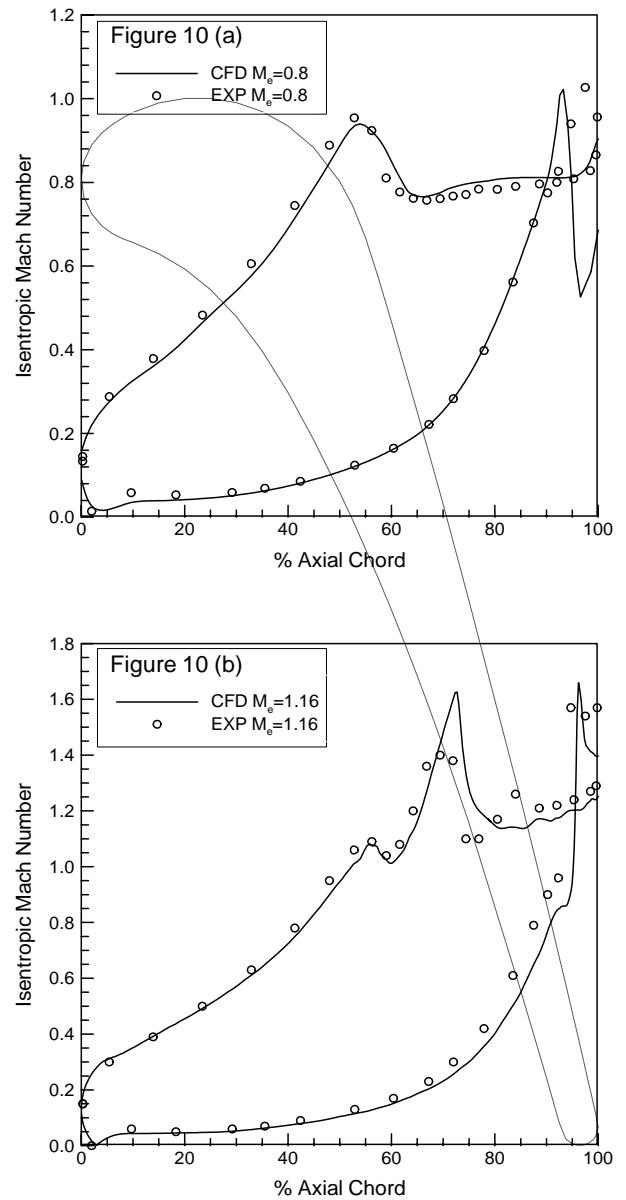


**Fig. 10 Experimental and inviscid CFD isentropic Mach number distribution for exit Mach 0.8 and 1.16.**

The most comprehensive base pressure correlation is that of Sieverding et al. (1980). The present results are compared with that correlation in Gostelow et al. (2009). As indicated in Fig. 12 the base pressure deficit is significantly under-predicted by the Sieverding correlation. This is thought to result from differing blade shapes in the trailing edge region.

### **Energy Separation**

Associated with the vortex shedding was a thermo-acoustic effect, which was particularly strong at high subsonic speeds. On a time-averaged basis, the stagnation temperature on the wake centre-line was found to be 12°C lower than for the incoming fluid. Meanwhile the stagnation temperature at the edges of the wake was 5°C higher than that of the incoming fluid. This effect had had a major adverse effect on the development of a new highly loaded turbine design. It was demonstrated by Carscallen et al. (1999) that this was a manifestation of the Eckert-Weise effect. In this thermo-

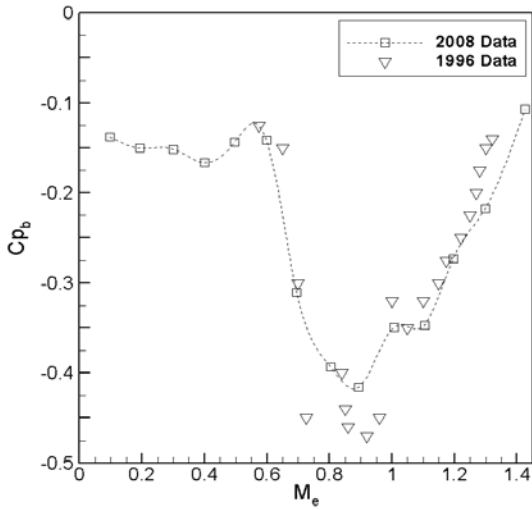


**Fig. 11 Base pressure as a function of discharge Mach number from two test series.**

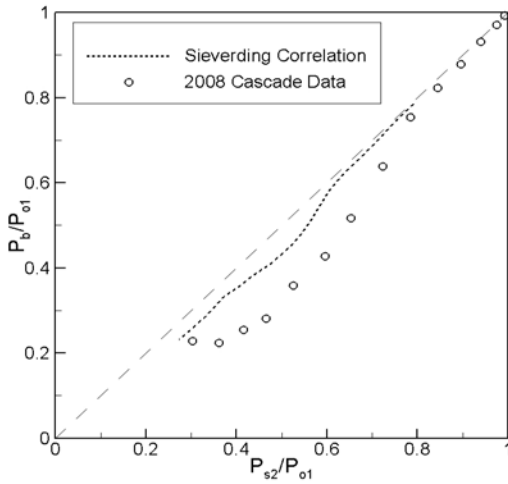


**Fig. 12 Measured base pressure coefficients compared with Sieverding correlation.**

acoustic effect, the vortex cores emerge colder than the surrounding fluid and are associated with hot spots at the edge of the wake.

On a time-averaged basis, this results in substantial total temperature redistribution. Investigation of this phenomenon involved measuring time-resolved temperature variations within the fluctuating wake and relating these to the previously observed time-average stagnation temperature variations. Hitherto attempts to obtain such time-resolved measurements had been frustrated by the inadequate bandwidth of the available temperature measurement instrumentation. Using innovative wide bandwidth temperature probes from Oxford University, the anticipated temperature fluctuations were detected and were of the order of 30K. This is what had been making it difficult to accurately establish the performance of the vane row. In the light of possible turbine efficiency implications of a few percent, it is important to be able to measure, average and model such flows accurately.

The frequency of vortex-shedding from the blades was of the order of 10 kHz and there was a requirement to make total temperature measurements with a bandwidth approaching 100 kHz for energy separation to be resolved and identified. This was

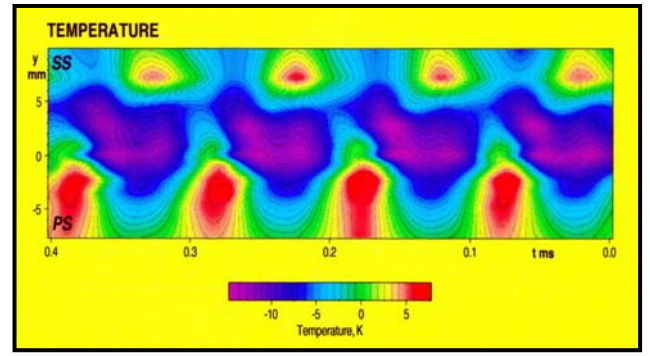


**Fig. 13 Time-resolved total temperature measurements in wake.**

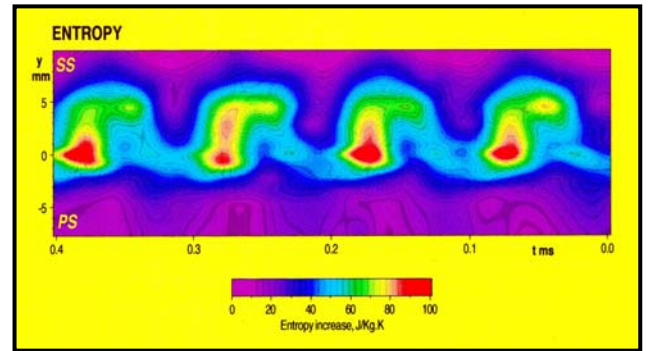


**Fig. 14 Time-resolved measurements of entropy increase.**

achieved using novel quartz rod mounted thin film gauges supplied by Oxford University (Buttsworth and Jones, 1998). A Kulite pressure transducer was mounted alongside the quartz rods, enabling total pressure to be measured simultaneously. It was therefore possible, using phase averaging, to construct contours of total pressure, total temperature and entropy increase at the measurement location in the vortex wake. As an example, the total

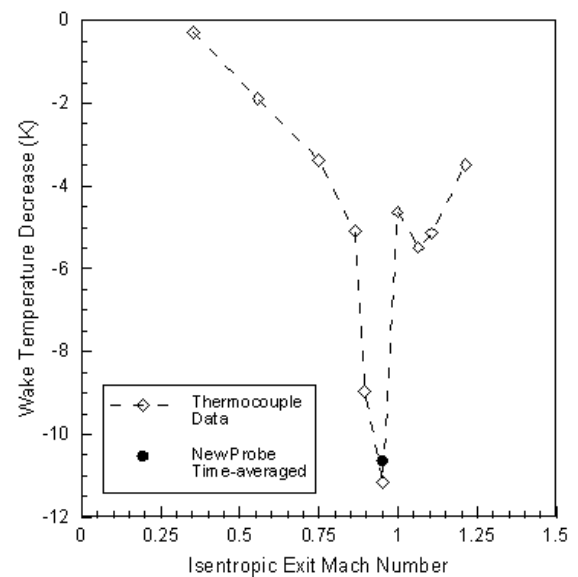


**Fig. 15 Comparison of original thermocouple measurements and time-average of new probe.**

temperature contours are shown in Fig. 13 and the entropy contours in Fig. 14. The relatively cool vortical structures on the wake centre-line are seen, as are the hot spots on the edge of the vortex wake. When time averaging is performed, the total temperatures are consistent with those measured using a slow response thermocouple, as shown in Fig. 15. These wide-bandwidth measurements represent the first time-resolved confirmation of the energy separation phenomenon.

A wide range of energy separation phenomena had been reviewed by Eckert who concluded that energy separation was primarily caused by pressure forces acting on the fluctuating curved streamlines with only a minor contribution from viscous forces. Acoustic effects tended to be an important ingredient of energy separation.

Because similar temperature redistributions were observed in planar and annular cascades, the vortex shedding effects described in this paper are equally applicable to annular cascades. The effects described are also likely to be present in rotating machines.

### **Exotic Shedding Modes**

The most common vortex shedding mode, that predicted by von Kármán, is not the only shedding mode. Not all vortex shedding takes form of a classical vortex street; a wide range of 'exotic' shedding modes exists. Carscallen and Gostelow (1994) discovered these anomalous patterns in the wakes of the NRC turbine cascade prompting an investigation of when they might occur. Two other applications were found, in the vortex-induced vibrations of bluff bodies and in research on oscillating airfoils. Findings from the vortex-induced vibration work of Williamson and Roshko (1988) and others clarified the shedding modes. Broadly corresponding designations from the field of vortex-induced vibration were identified in terms of the 2S, 2P, 2P\* and P+S definitions.

For some of the time, vortices were shed simultaneously from the two sides of the wake, rather than alternately. This behavior can be observed in Fig. 16 for the discharge Mach number of 1.09. Other modes were observed, in which vortex pairing appeared to be taking place on one side only as in Fig. 17. Since the passage shock behavior is determined by the vortex shedding mode, this anomalous behavior could have consequences for predicting the shock position, blade loading and dynamics. None of these additional transonic speed modes are explained by conventional stability theory. However, Ponta and Aref (2006) have performed an analysis that appears to predict the observed data well and extend them to a wider range of Reynolds numbers.

As the discharge Mach number becomes supersonic, the trailing edge shocks become oblique and the origin of the vortex street migrates from the trailing edge to the confluence of the two trailing edge shear layers. Previously available evidence had suggested that only free-stream disturbances are effective in provoking the vortex-shedding instability. In the present example, the visible existence and fixed location of acoustic waves precludes such a path for anti-symmetric upstream-travelling pressure waves. This has the effect of reducing the lateral distance between incipient vortices to the relatively short wake width at the downstream shock location. Nevertheless, significant free shear layer instabilities are thought to be propagated downstream through a Kelvin-Helmholtz mechanism.

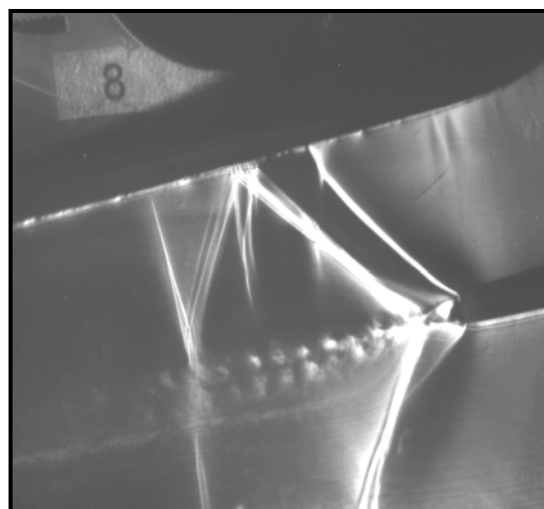


**Fig. 16 Schlieren view of vortex couples.**

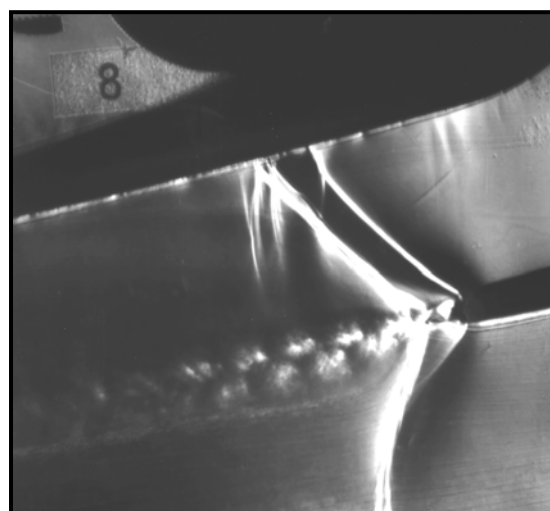


**Fig. 17 Schlieren view of vortex doublets.**

These phenomena, caused by vortex shedding, also play an important role in the loss-generation, due to low base pressures behind blades with thick trailing edges. The base pressure recovered significantly in transonic flows, where the vortex street changed its character. The anomalous vortex shedding patterns were therefore associated with a reduction in loss. They can also have a role in vortex-induced vibration of the resulting airfoil, which is effectively a bluff body.

Schlieren photographs from transonic cascades showed that the interaction between the base flow shear layers and the shock waves are the likely mechanism causing the changes in observed vortex-shedding patterns. There was a strong interaction between the downstream shock waves and the vortex shedding process but the coupling mechanism was not understood. Novel use of hydraulic analogy testing has helped clarify the dynamics of the interaction between the shock waves and the shed vortices. The above considerations suggest that the observed changes in vortex



shedding from the blunt trailing edges of the transonic cascade in the Mach number range between 0.97 and 1.2 are caused by a similar self-induced oscillation mechanism.

As shown in Figs. 16 and 17, shocks are generated at the confluence of the shear layers; the shocks interact with the shear layers. Findings, from Schlieren visualization, computational work and a separate hydraulic analogy experiment, have shown that the shock wave / wake interaction structure at the confluence of the shear layers is particularly dynamic and mobile. This results in the oscillatory flow causing the observed changes in vortex shedding.

## CONCLUSIONS

A wide range of vortex formation and shedding processes was identified in a transonic turbine nozzle cascade. Vortex formations included the expected horseshoe and secondary flow vortices and the surprising organized streamwise vorticity on the suction surface.

Cascade tests established that strong von Kármán vortex shedding occurred over the entire subsonic range of discharge Mach numbers. This resulted in strong base pressure deficits, causing high wake losses and energy separation in the wake. Time-resolved measurements of the Eckert-Weise energy separation phenomenon were made for the first time, explaining anomalies in the wake temperature variations.

At Mach numbers above unity, the von Kármán vortex street was found to be but one of a number of transient, yet distinct, shedding patterns. These corresponded to similar patterns observed in the field of vortex-induced vibration. The occurrence of similar changes in vortex shedding from transonic cascades suggests that the existence of an oscillating body is not a fundamental requirement. The wake instability can be caused by an oscillating pressure field. Shock-induced transonic flow oscillations could also change the modes of vortex shedding. The transonic cascade Schlieren photographs showed that the interaction between the base flow shear layers and the shock waves, which form at Mach numbers between 0.97 and 1.2, is the likely mechanism causing the changes in observed vortex-shedding patterns.

In these investigations on one high-turning nozzle vane cascade several distinct modes of vortex formation and shedding have been identified. The impact of some of these on turbine performance is potentially harmful. Furthermore, the presence of these disparate vortical structures clearly makes the fluid flow and heat transfer properties of the turbine blading challenging to interpret and predict.

## ACKNOWLEDGMENTS

Appreciation is expressed to Paul Hunt and to the M-10 team of NRC for running the facility and providing excellent support.

## REFERENCES

- Benner, M. W., Sjolander, S. A. and Moustapha, S. H., 1997, "Measurements of Secondary Flows in a Turbine Cascade at Off-Design Incidence," *ASME Paper 97-GT-382*.
- Buttsworth, D. R. and Jones, T. V., 1998, "A Fast Response Total Temperature Probe for Unsteady Compressible Flows," *Journal of Engineering for Gas Turbines and Power*, 120, 694-701.
- Carscallen, W. E. and Oosthuizen, P. H., 1988, "The Effect of Secondary Flow on the Redistribution of the Total Temperature Field Downstream of a Stationary Turbine Cascade," *AGARD CP-469*.
- Carscallen, W. E. and Gostelow, J. P., 1994, "Observations of Vortex Shedding in the Wake from Transonic Turbine Nozzle Vanes," *Proc. ISROMAC-5*, Kaanapali, HI.
- Carscallen, W. E., Fleige, H. U. and Gostelow, J. P., 1996, "Transonic Turbine Vane Wake Flows," *ASME Paper 96-GT-419*.
- Carscallen, W. E., Currie, T. C., Hogg, S. I. and Gostelow, J. P., 1999, "Measurement and Computation of Energy Separation in the Vortical Wake Flow of a Turbine Nozzle Cascade," *Journal of Turbomachinery*, 121, 4, 703-708.
- Cicatelli, G. and Sieverding, C. H., 1996, "The Effect of Vortex Shedding on the Unsteady Pressure Distribution around the Trailing Edge of a Turbine Blade," *ASME Paper 96-GT-359*.
- Denton, J. D., 1993, "Loss Mechanisms in Turbo-machines," *Journal of Turbomachinery*, 115, 621-56.
- da Vinci, Leonardo, 1506-1510, *Codex Leicester*.
- Eckert, E. R. T. and Weise, W., 1943, "Messungen der Temperaturerteilung auf der ober Fläche Schnell Angeströmter Unbeheizter Körper," *Forsch. Ing. Wesen*. Vol. 13, pp. 246-254.
- Görtler, J., 1955, "Three-Dimensional Instability of the Stagnation Point Flow with Respect to Vortical Disturbances," (in German). In *50 Years of Boundary Layer Research*, ed. Görtler and Tollmien, Vieweg, Braunschweig, 14, 17, 304-14.
- Gostelow, J. P., Mahallati, A., Andrews, S. A. and Carscallen, W. E., 2009, "Measurement and Computation of Flowfield in Transonic Turbine Nozzle Blading with Blunt Trailing Edges," *ASME Paper GT2009-59686*.
- Hodson, H. P. and Dominy, R. G., 1987, "The Off-Design Performance of a Low-Pressure Turbine Cascade," *Journal of Turbomachinery*, 109, 201-209.
- Kestin, J. and Wood, R. T., 1970, "On the Stability of Two-Dimensional Stagnation Flow," *J. Fluid Mech.* 44, 461-479.
- Lawaczeck, O. and Heinemann, H. J., 1976, "von Kármán Streets in the Wakes of Subsonic and Transonic Cascades," *AGARD CP-177*.
- Mee, D. J., Baines, N. C., Oldfield, M. L. G. and Dickens, T. E., 1992, "An Examination of the Contributions to Loss on a Transonic Turbine Blade in Cascade," *Journal of Turbomachinery*, 114, 155-62.
- Ponta, F. and Aref, H., 2006, "Numerical Experiments on Vortex Shedding from an Oscillating Cylinder," *Journal of Fluids and Structures*, 22, 327-344.
- Schulz, H. D. and Gallus, H. D., (1988), "Experimental Investigation of the Three-Dimensional Flow in an Annular Compressor Cascade," *Journal of Turbomachinery*, 110, 467-478.
- Sieverding, C. H., Stanislas, M. and Snoeck, J., 1980, "The Base Pressure Problem in Transonic Turbine Cascades," *Journal of Eng. for Power*, 102, 711-718.
- Weber, A., Schreiber, H.-A., Fuchs, R. and Steinert, W., 2002, "3D Transonic Flow in a Compressor Cascade with Shock-Induced Corner Stall," *Journal of Turbomachinery*, 124, 3, 358-366.
- Williamson, R. G. and Moustapha, S. H., 1986, "Annular Cascade Testing of Turbine Nozzle at High Exit Mach Numbers," *Journal of Fluids Engineering*, 108, 313-320.
- Williamson, C. H. K. and Roshko, A., 1988, "Vortex Formation in the Wake of an Oscillating Cylinder," *Journal of Fluids and Structures*, 2, 355-381.